Emplacement P-T conditions of granitoids from the NW-part of the Malayer-Boroujerd plutonic complex, W Iran

Hadi Yeganehfar[1], Reza Deevsalar[2,*]

1- Department of geology, Payame Noor University (PNU), P.O.Box: 19395-4697 Tehran, Iran.

2- Department of geology, Faculty of science, Tarbiat Modares University, Iran.

* Corresponding Author: deevsalar@gmail.com

Received: 13 March, 2016 / Accepted: 08 December 2016 / Published online: 28 December 2016

Abstract

The application of different geothermometer and geobarometer for selected granitoids from the NW-part of the Malayer-Boroujerd plutonic complex (NW MBPC) indicates they were sourced at pressures below 14 kb and emplaced at 8 to 4 kb. The results show relatively three areas of P-T condition for emplacement of NW MBPC granitoids: (1) Low- P and T (P< 5kb and T < 680°C) for Garnet-bearing monzogranite (Grt- MG) and quartz sample diorite, (2) High- P and T (~ 8 kb and T = 721°C) for garnet-bearing alkali granite (Grt- Alk Gr), and (3) Low- P and high T (P< 5kb and T > 750°C) for hornblende-bearing I-type granite (Hbl-granite) and hornblende-free S-type granite. The P–T estimation suggests that the hydrous felsic magma with S-type affinity were formed either by melting of deep crustal components followed by extensive assimilation of muscovite-bearing sediments or direct melting of muscovite-bearing metapelitic rocks at low pressure, both emplaced within muscovite-free domain of granitic system. The hydrous I-type felsic magmas which were mainly formed by melting of lower crustal materials cut the granite solidus at low pressure and show little evidence for assimilation of crustal components at emplacement level. The calibrations applied for NW MBPC granitoids indicates an important role for muscovite as H2O-supplier for felsic parent magma. The temperature increasing gradient against pressure for this region is greater than standard gradient for subduction zone indicating the intrusion of mantle-derived mafic magma into the crust or local thickening of continental crust.

Keywords: Geothermobarometery; Granitoids; Level of emplacement; Muscovite; NW MBPC; Sanandaj-Sirjan Zone.

1- Introduction

Within the crust heat from the underlying mafic magma is transferred by conduction and aqueous fluids are the main media carry temperature and mass towards shallower depth. This is an efficient way to produce crustal melt from fertile upper crust. Advective heat transfer by mantle-derived magmatism increases the geothermal gradient in subduction zone setting. When mantle-derived basaltic melt reach to the bottom of continental crust, it is feasible to transfer both mass and heat to the lowermost crust (e.g. Tatsumi and Suzuki 2009, Reiners et al. 1995) which would generate evolved magmas either by crustal anatexis (e.g. Smith and Leeman 1987, Petford and Atherton 1996, Fornelli et al. 2002, Sisson et al. 2005) or closed system fractionation (Sisson and Grove 1993; Kawamoto 1996; Grove et al. 2003; Pichavant and Macdonald 2007; Tatsumi and Suzuki 2009).

Geological thermometers and barometers have been widely applied to metamorphic rocks to reconstruct both palaeogeotherm and P-T condition of generation and emplacement of granitic magmas (Pattison et al., 1982). The petrogenesis and geochemistry of granitic magmas are mainly controlled by P-T conditions in their source region and emplacement depth (Clemens 1984; Wickham 1987; Vielzeuf and Holloway 1988). So, the extensive melting of deep or shallow crustal components and emplacement of large granitic plutons provides important information on the thermal evolution and P-T conditions for different tectonic setting, especially, continental subduction zone setting (e.g. Pin and Vielzeuf 1983; Wickham 1987).

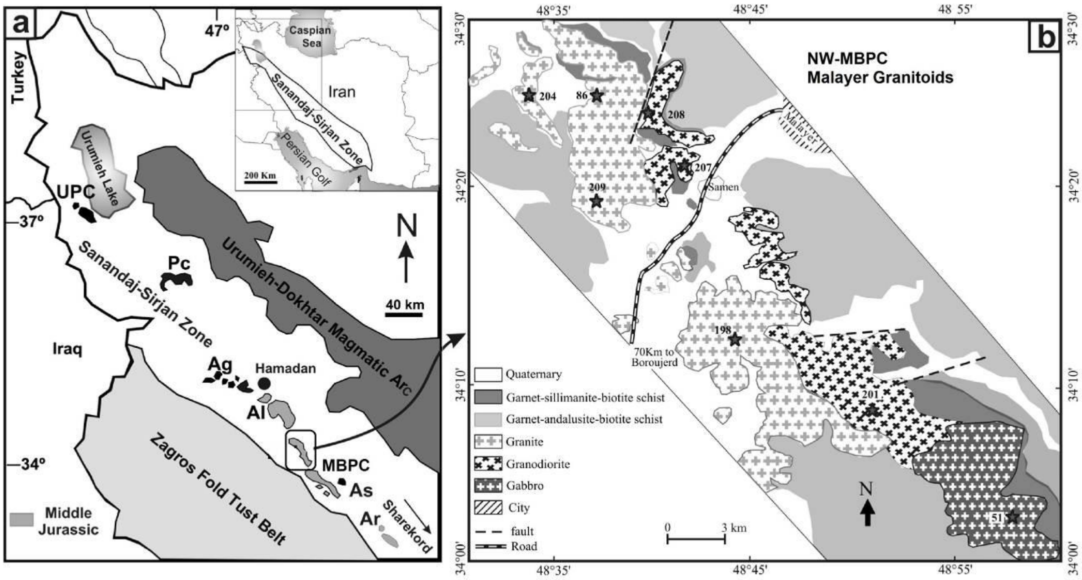

Figure 1 A) West and northwestern part of Iran map, showing three major elements of the Zagros Orogen (Ahadnejad 2013). The NW-MBPC is enclosed by rectangle. B) Different igneous rocks in the NW-MBPC. The most important plutonic bodies in the Sanandaj-Sirjan Zone, Iran (modified from Emami et al. 1994). Inset map: Sanandaj-Sirjan Zone position in Iran. UPC = Urumieh plutonic complex (Ghalamghash et al. 2009a, b); PC = Pichagchi (Kholghi Khasraghi and Vossoughi Abedini 2004); AG = Almogholgh (Valizadeh and Cantagrel 1975); AL = Alvand (Valizadeh and Cantagrel, 1975; Braud, 1987; Baharifar et al. 2004; Shahbazi et al. 2010); MBPC = Malayer-Boroujerd Plutonic complex (Ahadnejad et al. 2010; Deevsalar et al., 2014; Masoudi et al. 2002; Ahmadi-Khalaji et al. 2007); AS = Astaneh (Massoudi et al. 2002); Ar = Aligudarz (Esna-Ashari et al. 2012). b. Location and numbers of the samples from NW MBPC (Malayer pluton).

We have systematically determined the P-T conditions of equilibration of mineral assemblages in Middle Jurassic age granitic rocks (Ahmadi-Khalaji et al. 2007; Ahadnejad et al. 2010) from the Malayer-Boroujerd plutonic complex (MBPC), using available geothermometers and geobarometers. These data allow the P-T condition and the mechanism of generation of granitic magma to be constrained and Middle Jurassic geotherms be constructed. According to Mohajjel and Ferguson (2014), the MBPC belong to Middle Jurassic Qorveh-Aligudarz arc which located in Northern Sanandaj-Sirjan Zone (N-SSZ), W Iran.

Although, geothermobarometric calculations for plutonic rocks and especially granitoids are not easy, many researchers have used mineral thermobarometric methods to granitoid rocks (Vyhnal et al. 1991; Schmidt 1992; Lissenberg et al. 2004). Since, there are few suitable mineral assemblages in granitoid rocks for thermobarometry, the pressure and temperature estimation in those studies is, based mainly on Al-in-hornblende barometry (Hammarstrom and Zen 1986; Hollister et al. 1987; Schmidt 1992) and amphibole-plagioclase thermometry (Holland and Blundy 1994; Blundy and Holland 1990).

2- Analytical methods and procedure

Among unaltered hand specimens collected by scrutinized field studies, numbers of representative samples were selected from each unites, based upon the presence of primary magmatic minerals including biotite, apatite, zircon and coexisting garnet-biotite, amphibole-plagioclase. Mineral major element values were determined by EPMA, (device model Jeol JXA-8200R) in the Institute of Mineralogy and Petrology, Federal University of Zurich (ETHZ, Switzerland) with beam voltage of 15kv, beam current 20ne and counting time of 40s. The standards used in the EDS system are natural quartz for Si, natural anorthite for Al, natural periclase for Mg, natural albite for Na, natural orthoclase for K, natural hematite for Fe, synthesized wollastonite for Ca, rhodonite for Mn and natural ilmenite for Ti. All analyzed lines for each element were the K-alpha line. Matrix corrections were made using standard ZAF techniques.

3- Geological setting

The study area is a NW-SE trending complex with 35 km length and up to 10 km width. The MBPC is located in the northern part of the Sanandaj-Sirjan Zone (SSZ). The SSZ extends for 1500 km from Taurus orogenic belt in Turkey (in NW Iran) to the Esfandagheh (in SE Iran) (Fig. 1), compose internal magmatic zone of the Zagros Orogen. As shown in Fig. 1, it lies parallel to the external magmatic zone of Zagros Orogen, i.e. Urumia-Dokhtar Magmatic Zone (UDMZ) and continues westward into Turkey and Syria and eastward into the Bajgan Durkan complexes of the Makran (McCall 2002). The MBPC is composed of Middle Jurassic age felsic and mafic intrusive rocks (Ahmadi-Khalaji et al. 2007; Ahadnejad et al. 2010; Deevsalar et al. 2017). Felsic granitic rocks are prevalent rock types within the MBPC. Similar to adjacent areas in SSZ, almost all felsic granitic magma intruded into the high levels of MBPC continental crust, were emplaced within metapelitic country rocks (i.e. spotted schists and hornfelse). In some localities refractory minerals and restites including andalusite and garnet have been found within granitoids. The NW MBPC (i.e. Malayer granitoids in Ahadnejad et al., 2008, 2010, 2011) granitoids compositions range from seyeno-monzogranite to granodiorite-tonalite composition. Granodiorite is dominant especially in NW MBPC and less abundant rock types are hyperalkaline granites, garnet-bearing monzogranites and quartz diorites. In the literature (e.g. Deevsalar et al. 2009; Ahadnejad et al. 2010, 2011), their formation attributed either to crustal anatexis or assimilation fractional crystallization processes. They found in both S- and I-type affinities, however they are mainly S-type in the areas those representative samples were collected. Biotite is the main mafic mineral in these rocks, especially in granodiorites. Anorthitic plagioclase, alkali feldspare, quarts ± amphibole, zircon and apatite and garnet are other primary magmatic minerals constitute the representative samples.

4- Geobarometery

The presence of primary garnet in some samples from the NW MBPC granitoids provides constraints on pressure of the source region. The stability field for magmatic garnet in water-saturated granitic melts is greater than 13.99 kb (Schmidt and Thompson 1996; Schmidt and Poli 2004), therefore the garnet-bearing monzogranite and garnet-bearing hyperalkaline granites (Ahadnejad, 2011) may have originated from this depth. In this regards, lacking of evidence for garnet in the hornblende-bearing granites and quartz diorite suggest that the plutons were generated at pressures <13.99 kb.

4.1- Quartz-Albite-Orthose (Q-Ab-Or) cotectic in a haplogranitic system

Many of the researchers apply Quartz-Albite-Orthose diagram to correlate experimental data with composition of natural rocks, however some of them use it with caution (Rolinson, 1993). This graph suggests different crystallization depth and pressure for the NW MBPC granitoids, as the syenogranites, monzogranites and granodiorites place close to the H2O-saturated cotectic at 1-10 kb, 0.5-5 kb and 3-10 kb respectively. Fig. 2 shows the NW MBPC granitoids on Q-Ab-Or diagram in which the cotectic points change by PH2O (Schairer and Bowen 1935; Tuttle and Bowen 1958; Luth et al. 1964; Huang and Wyllie 1975).

4.2- Al-in-hornblende barometer

The NW MBPC granitoids contain a mineral assemblage (quartz, alkali feldspar, hornblende and plagioclase) and high phenocryst content (50-75 vol %) are suitable for application of the Al-in-hornblende barometer (Schmidt, 1992). In this regards, we used rim compositions of hornblende grains in contact with quartz and alkali feldspar. Worth to note that, the Al-in-hornblende barometer was applied to unaltered magmatic amphiboles with $^{IV}Al < 0.8$.

Table 1) Major element composition of 12 analytical points on amphiboles from the NW MBPC granitoids.

Sample	51-			86-			198-			201-		
	#1	#2	#3	#1	#2	#3	#1	#2	#3	#1	#2	#3
Petrology	Q-Di			SG			MG			Gd		
SiO_2	50.38	50.18	50.16	51.56	51.45	51.23	51.62	51.14	50.83	51.19	51.15	51.11
TiO_2	0.73	0.78	0.71	0.50	0.52	0.52	0.50	0.51	0.54	0.51	0.52	0.52
Al_2O_3	6.83	6.47	6.85	8.30	7.31	7.11	8.32	7.56	6.89	7.25	6.82	6.12
FeO	13.52	13.62	6.85	12.42	12.78	12.89	13.01	13.41	13.71	13.01	13.01	13.42
MnO	0.30	0.30	0.30	0.20	0.29	0.29	0.24	0.24	0.30	13.20	0.32	0.33
MgO	13.11	13.11	13.22	12.38	12.61	12.82	12.51	12.06	13.29	0.31	12.98	13.22
CaO	10.25	10.25	10.85	9.43	10.01	10.16	9.11	9.72	9.81	10.11	10.49	10.74
Na_2O	0.91	0.73	0.82	1.34	1.30	1.31	1.14	1.13	0.98	0.93	1.01	0.93
K_2O	0.54	0.51	0.53	0.76	0.76	0.76	0.77	0.76	0.71	0.53	0.72	0.71
Total	96.57	95.95	90.29	96.89	97.05	97.09	96.98	96.54	97.07	97.04	97.03	97.10
TSi	7.27	7.28	7.72	7.39	7.42	7.39	7.35	7.40	7.27	7.29	7.38	7.39
TAl	0.73	0.72	0.28	0.61	0.58	0.61	0.65	0.60	0.73	0.71	0.62	0.61
TFe^{+3}	0.00	0.00	0.00	0.00	0.00	0.00	0.00	0.00	0.00	0.00	0.00	0.00
TTi	0.00	0.00	0.00	0.00	0.00	0.00	0.00	0.00	0.00	0.00	0.00	0.00
Sum_T	8.00	8.00	8.00	8.00	8.00	8.00	8.00	8.00	8.00	8.00	8.00	8.00
CAl	0.43	0.39	0.96	0.79	0.66	0.60	0.74	0.69	0.43	0.60	0.54	0.43
CCr	0.00	0.00	0.00	0.00	0.00	0.00	0.00	0.00	0.00	0.00	0.00	0.00
CFe3	0.62	0.67	0.00	0.31	0.22	0.26	0.57	0.33	0.77	0.55	0.30	0.35
CTi	0.08	0.09	0.08	0.05	0.06	0.06	0.05	0.06	0.06	0.05	0.06	0.06
CMg	2.82	2.84	3.03	2.65	2.71	2.76	2.66	2.60	2.83	2.77	2.79	2.85
CFe2	1.02	0.98	0.88	1.18	1.32	1.30	0.98	1.30	0.87	1.00	1.27	1.27
CMn	0.04	0.04	0.04	0.02	0.04	0.04	0.00	0.03	0.04	0.04	0.04	0.04
CCa	0.00	0.00	0.00	0.00	0.00	0.00	0.00	0.00	0.00	0.00	0.00	0.00
Sum_C	5.00	5.00	5.00	5.00	5.00	5.00	5.00	5.00	5.00	5.00	5.00	5.00
BMg	0.00	0.00	0.00	0.00	0.00	0.00	0.00	0.00	0.00	0.00	0.00	0.00
BFe2+	0.00	0.00	0.00	0.00	0.00	0.00	0.00	0.00	0.00	0.00	0.00	0.00
BMn	0.00	0.00	0.00	0.00	0.00	0.00	0.00	0.00	0.00	0.00	0.00	0.00
BCa	1.59	1.59	1.79	1.45	1.55	1.57	1.39	1.51	1.50	1.56	1.62	1.66
BNa	0.26	0.21	0.21	0.37	0.36	0.37	0.31	0.32	0.27	0.25	0.28	0.26
Sum_B	1.84	1.80	2.00	1.82	1.91	1.94	1.70	1.83	1.78	1.81	1.91	1.92
ACa	0.00	0.00	0.00	0.00	0.00	0.00	0.00	0.00	0.00	0.00	0.00	0.00
ANa	0.00	0.00	0.03	0.00	0.00	0.00	0.00	0.00	0.00	0.00	0.00	0.00
AK	0.10	0.09	0.10	0.14	0.14	0.14	0.14	0.14	0.13	0.10	0.13	0.13
Sum_A	0.10	0.09	0.14	0.14	0.14	0.14	0.14	0.14	0.13	0.10	0.13	0.13
Sum_cat	14.94	14.89	15.14	14.96	15.05	15.08	14.84	14.97	14.91	14.91	15.04	15.06
CCI	0.00	0.00	0.00	0.00	0.00	0.00	0.00	0.00	0.00	0.00	0.00	0.00
CF	0.00	0.00	0.00	0.00	0.00	0.00	0.00	0.00	0.00	0.00	0.00	0.00
Sum_oxy	23.00	23.00	23.39	23.00	23.00	23.00	23.00	23.00	23.00	23.00	23.00	23.00

All calculations were made on the basis of Fe_{total} = FeO and 23 oxygen atoms (Table 1). The estimated pressures for selected intrusions range between 3.7–2.6 kb, corresponding to a depth of about 21–10 km (Fig. 3). Higher pressure estimates (> 3 kb) were obtained for the quarts diorite intrusion (Q-Di, Table 1) and those granites containing Al_2SiO_5 polymorphs (4-5 kb). Despite of lower pressure estimated by this calibration, the result is consistent with pressure estimated in H_2O-saturated cotectic from Q-Ab-Or haplogranitic system. Considering the confidence limit of the error for Al-in-hornblende barometers (~ 0.3 kb), this calibration yields satisfactory results for pressure conditions relevant to this study. Furthermore, pressure estimate using Al-in-hornblende barometry is trustable because of low Fe^{2+}/Fe^{2+}+Mg ratios (< 0.4) in amphiboles from the NW MBPC granitoids relative to values recommended by Anderson and Smith (1995) (i.e. $Fe^{\#} < 0.65$).

Fine-grained to porphyritic and granophyric textures and sharp contacts with metapelitic country rocks is in good agreement with pressure estimated by Schmidt's barometer indicating high-level emplacements of these granitoids.

4- Grothermometery

4.1- Zircon and apatite saturation geothermometers

The accessory minerals play important role in the petrogenesis of the igneous rocks, because of their ability to incorporate and retain trace elements and isotopic information. In granitic system thorough understanding the role of early crystallized accessory minerals is crucial to constrain petrogenesis and physical condition of the magmagenesis.

Zircon is one of the important accessory mineral in both differentiated and crustal-derived granitic system. However they crystallize in early stage of magmatic fractionation, but the low solubility of crystalline zircon ($ZrSiO_4$) in felsic and non-peralkaline magmas, similar to those in NW MBPC, makes it possible the presence of inherited zircon crystals in those crustal granitoids. Zircon saturation and crystallization depends basically on temperature and melt composition, makes it an indispensable tool for petrologist in deciphering the temperature at which parent magma was started to crystallization (Watson and Harrison 1983; Hanchar and Watson 2003). In this regards, we could calculate the liquidus temperature by using Zr concentration in each samples. We applied Saturnin program in GCDkit software (Janoušek et al. 2006) to calculate zircon saturation temperature. The results for 48 samples are represented in Table 2. Calculated zircon saturation temperature is around 777°C.

Table 2) Emplacement temperatures estimated by zircon and apatite saturation thermometers.

Sample name	31	38	40	44	54	56	61	68	73	76	77	80	87	90	91	93	101	106
T_{Zr}.sat.°C	903	742	783	845	808	818	754	765	806	800	738	756	752	756	749	741	677	739
T_{Ao}.sat.°C.	-	-	986	841	713	-	-	712	0	622	-	702	704	-	1026	-	-	-
Sample	110	112	116	117	125	126	127	133	134	149	150	152	154	155	156	157	159	161
T_{Zr}.sat.°C	728	811	766	734	777	757	789	747	761	792	755	800	819	692	705	829	698	798
T_{AD}.sat.°C.	-	881	399	-	-	832	680	-	823	682	599	-	-	-	-	838	-	468
Sample	163	164	174	175	183	186	187	188	189	191	192	193	**Average**					
T_{Zr}.sat.°C	776	846	735	809	815	824	853	825	799	830	785	728	**777**.°C					
T_{AD}.sat.°C.	808	627	-	-	-	805	734	818	-	0	0	872	**753**.°C					

Apatite is very important accessory phase in silicate system that preferentially incorporates LREE even in minor modal abundances. Using experimental data, Harrison and Watson (1984) suggested a model for apatite behavior in crustal melts within different temperature and silica contents. However, sub-aluminous granitoids yielded good results in this model but the calculated apatite saturation temperature in peraluminous system was of course unreliable. However, Janoušek et al. (2006) argued that apatite saturation thermometer is not a robust tool in both felsic metaluminous and peraluminous system. For comparison, we calculated the emplacement temperatures by apatite saturation thermometer in GCDkit software (Janoušek et al. 2006). In the case of NW MBPC granitoids, the P concentration yield average temperature about 753°C near to that estimated by zircon saturation geothermometer for incipient crystallization of apatite (Table 2).

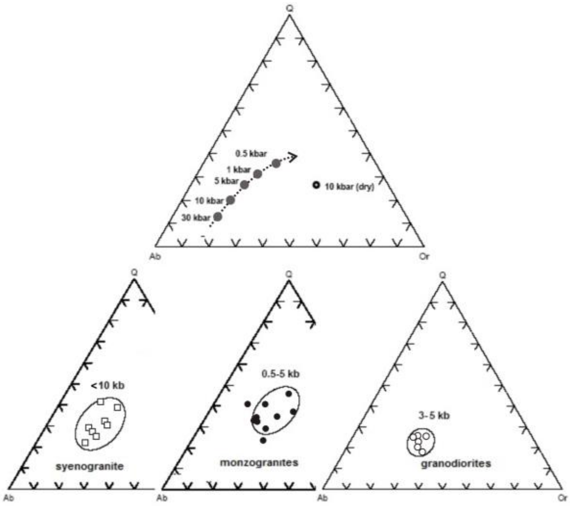

Figure 2) CIPW Quartz-Albite-Orthose diagram for the NW MBPC granitoids (Hbl-free granitoids) is indicating crystallization at different pressures.

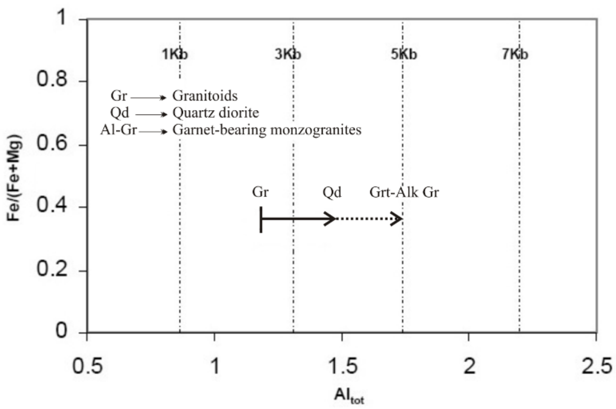

Fig. 3 Altot vs Fe^{2+}/Fe^{2+} + Mg plot (Schmidt 1992). It shows range of crystallization pressure estimated by Al-in Hornblende barometer for the NW MBPC granitoids (Hbl-bearing quartz diorite to granodiorites).

4.2- Ti-in-Biotite geothermometer (TIB)

The presence of few samples/locations containing refractory Al_2SiO_5 polymorphs in NW MBPC granitoids indicate melting of metapelitic/metamorphic wall rocks by ascending granitic magmas. The Ti-in-biotite geothermometer of Henry et al. (2005) which is based on the Ti-saturation surface of near-isobaric natural biotite data for peraluminous metapelites equilibrated at 4-6 kb, applied for these samples. We selected those samples met the criteria for TIB geothermometry defined by Henry et al. (2005). According to these criteria, limited numbers of crustal-derived S-type granitoids containing refractory metapelitic minerals (andalusite or garnet) and biotite with rutile inclusions and ilmenite were qualified for further consideration. In TIB thermometer, temperatures can be determined either by plotting biotite Ti and Mg/(Mg+Fe) values on the simple binary diagram or by calculating T-values from the expression: $T=([\ln(Ti)-a-c(XMg)^3]/b)^{0.333}$. In this formula, T is temperature in °C, Ti is the apfu normalized to 22 oxygen, XMg is Mg/(Mg+Fe), and the a, b and c parameters are constant parameters given in Henry et al. (2005). Using equation represented above, the equilibrium temperature for S-type peraluminous granites from the NW MBPC which contain andalusite or garnet is around 610-680 °C (Fig. 4).

4.3- Geothermometry by Mineral pairs

Mineral pairs with different paragenesis provide information about physical condition of crystallization. The following assemblages and calibrations have been used to estimate magmatic or subsolidus mineral equilibration temperatures:

1- Amphibole-plagioclase geothermometer: amphibole is a ubiquitous mineral phase in calc-alkaline plutonic rocks and amphibolite grade metamorphic rocks. Because of stability in hydrous environment, it could be found as the main primary mineral in granitoids, especially those with basic composition containing calcic plagioclase. Holland and Blundy (1994) and Blundy and Holland (1990) developed a thermometer based on the $A1^{iv}$ content of amphibole coexisting with plagioclase in silica saturated rocks. The application of amphibole-plagioclase calibration for granitoids from

NW MBPC yields temperatures of equilibration for hornblende-plagioclase assemblages around 649-724°C with uncertainties of around ±30°C (Table 3). This thermometer was not applied in samples containing highly calcic plagioclase (X_{An} > 90). The highest and lowest subsolidus temperatures estimated by primary amphibole-plagioclase pairs are related to syenogranite and granodiorite-tonalite samples, respectively.

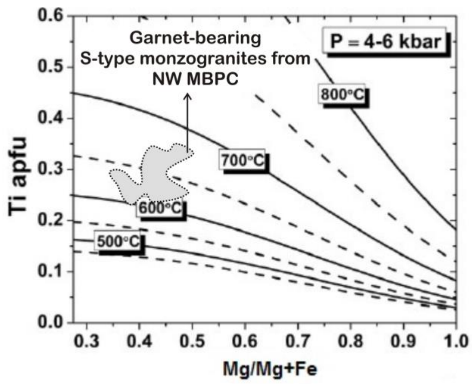

	Coefficients	a	b	c
Sample	Petrology	Ti	XMg	T (°C)
11	Monzogranite	0.256	0.47	633
13	Granodiorite	0.294	0.43	649
34	Granodiorite	0.309	0.44	659
		0.27	0.43	635
72	Syenogranite	0.258	0.44	628
		0.264	0.38	609
108	Syenogranite	0.247	0.37	609
		0.326	0.43	666
		0.258	0.36	634
122	Granodiorite	0.304	0.43	655
		0.281	0.44	643
153	Monzogranite	0.319	0.45	666
		0.339	0.48	681
163	Tonalite	0.305	0.43	656

Figure 4) Equilibrium temperatures estimated by TIB thermometer in garnet-bearing monzogranite.

2- Biotite-garnet thermometer: Although this calibration was initially suggested for metapelitic rocks of amphibolite facies, but it revised and recalibrated several times and developed further for other rock types. Ferry and Spear (1978) recalibration are among the most commonly used one. This thermometer works based on the exchange of Fe^{+2} and Mg^{+2} between garnet and biotite which can be written as a reaction among the Fe and Mg end-members of these minerals:

$$Fe_3Al_2Si_3O_{12} + KMg_3AlSi_3O_{10}(OH)_2 = Mg_3Al_2Si_3O_{12} + KFe_3AlSi_3O_{10}(OH)_2$$

Primary garnets are found coexisting with primary magmatic biotite in some outcrops of hyperalkaline granites within NW MBPC. We applied Ferry and Spear (1978) calibration for garnet-biotite-bearing granites from the NW MBPC.

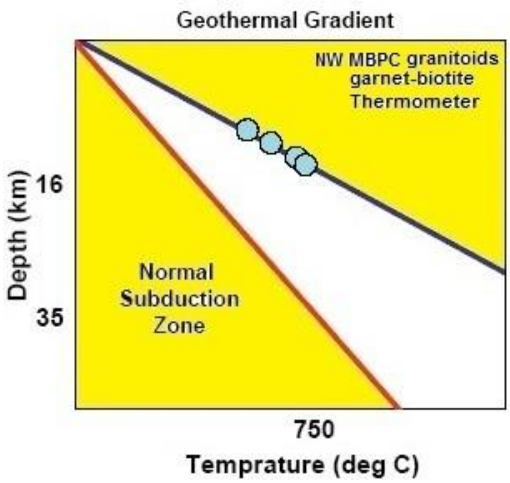

Figure 5) Geothermal gradient in MBPC compared with that in a normal subduction zone setting (Hacker et al. 2008). Filled circle shows the NW MBPC granitoids on their relevant geotherm.

This calibration yields satisfactory results for P-T conditions relevant to this study. Biotite-garnet assemblage gives temperature estimates around 721°C (at P~ 8kb) consistent with field evidence of crustal partial melting (high proportion of refractory minerals in the restitic or micaceous enclaves) and the results achieved by other calibrations. The major element composition of three pairs of garnet and biotite and the results of temperature estimation are given in Table 4.

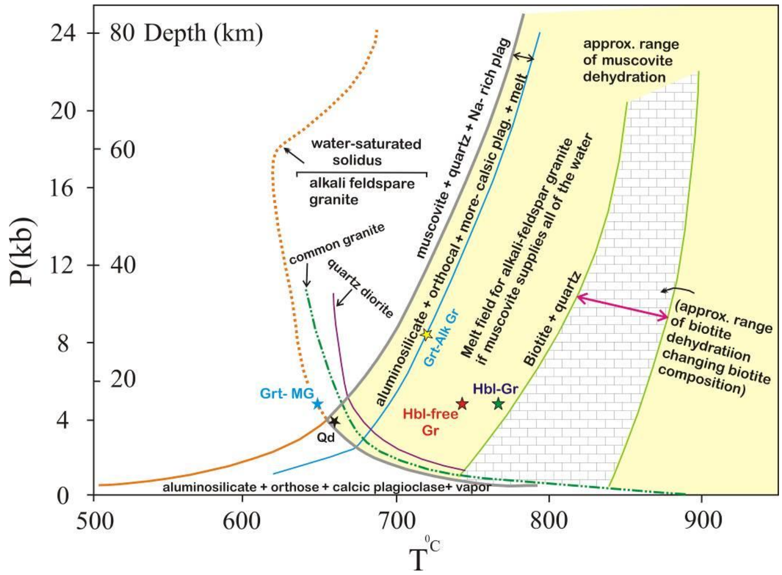

Figure 6) The NW MBPC granitoids are shown on the P-T projection for granitic system.

Table 3) Equilibrium temperatures estimated by amphibole-plagioclase thermometers.

Sample	51 -#1	Amphibole 201-#1	198-#1	86-#1
Petrology	Qd	MG	Gd	SG
SiO_2	50.380	48.228	49.057	50.690
TiO_2	0.730	0.288	0232	0.501
Al_2O_3	6.830	9.115	8.252	9297
FeO*	13.520	14.641	15.352	13.420
MgO	13.110	12.584	12.612	12.380
MnO	0.300	0.238	0.404	0.201
CaO	10.250	11.973	11.385	9.428
Na_2O	0.910	0.957	0.691	1.342
K_2O	0.540	0.263	0.373	0.762
Sum	96.570	98.29	98.36	98.02
Plagioclase				
XAb	45	65	46	51
XAn	50	34 6	52 9	47
Sum cations	15.121	15.183	15.166	15.141
Thermometry based on arbitrary pressure				
P(kb)	3.7	6	6	6
T (C) HB'90	661.3	664.1	690	628.9
Results based on Schmidt pressure				
P(kb)	2.59	4.26	3.68	4.47
T(C) HB'90	650	687.3	724	649.7

BH refers to Blundy and Holland (1990)
Hbld-Plag thermometry calibration reaction:
edenite + 4 quartz = tremolite + albite

5- Petrogenetic usage

As shown in Fig. 6, the NW MBPC granitoids plot in the muscovite-free domain of the P-T projection for granitic system (Table 5). It suggests an important role for dehydration melting of muscovite-bearing crustal components in the generation of the MBPC granitoids, especially those we are applied for P-T estimation. According to Fig. 6, the granitoids from the NW MBPC were emplaced in three distinct P-T condition, including, (1) Low- P and T: Garnet-bearing monzogranite (Grt-MG) and quartz diorite plot close to water saturated solidus and ordinary granite's solidus at P < 5 kb and T < 680 °C, (2) High- P and T: garnet-bearing alkali granite (Grt- Alk Gr) cut the granite solidus at highest pressure about ~ 8 kb and T = 721 °C, and (3) Low- P and high T: hornblende-bearing I-type granite (Hbl-granite) and hornblende-free S-type granite place below muscovite stability field at highest T (> 750 °C).

Table 4) Major element composition and temperatures estimated by garnet-biotite thermometer.

Samples	70#1	70#1	70#2	70#2	70#3	70#3
Petroloqv	Alkali-granite					
Minerals	garnet	biotite	garnet	biotite	garnet	biotite
	Wt%					
SiO_2	37.04	33	37.12	32.87	37.09	32.91
TiO_2	0.11	2.14	0.12	2.21	0.11	2.15
Al_2O_3	20.59	17.7	20.67	17.4	20.61	17.55
Cr_2O_3	0	0	0.001	0	0	0
Fe2O3	3.38	2.36	3.4	2.27	3.44	3.31
FeO	30.33	21.24	30.39	21.53	30.45	21.41
MnO	3.54	0.19	3.51	0.18	3.49	0.21
MgO	3.5	8.09	3.35	8.22	3.47	8.15
CaO	1.21	0.27	1.16	0.35	1.19	0.31
Na_2O	0.1	0.14	0.06	0.05	0.09	0.12
K_2O	0.2	11.3	0.13	11.1	0.17	11.27
H_2O	0.02	3.14	0.01	3.17	0.1	3.2
Totals	100.02	99.57	99.921	99.35	100.21	100.59
	a.p.f.u.					
Si	2.970	4.799	2.977	4.793	2.936	4.752
Ti	0.007	0.234	0.007	0.242	0.007	0.233
Al	1.947	3.035	1.955	2.991	1.943	2.987
Cr	0.000	0.000	0.000	0.000	0.000	0.000
Fe+3	0.204	0.259	0.205	0.249	0.207	0.360
Fe+2	2.034	2.583	2.039	2.625	2.036	2.585
Mn	0.240	0.023	0.238	0.022	0.236	0.026
Mg	0.418	1.753	0.400	1.786	0.414	1.754
Ca	0.104	0.042	0.100	0.055	0.102	0.048
Na	0.016	0.039	0.009	0.014	0.014	0.034
K	0.020	2.097	0.013	2.065	0.017	2.076
OH	0.011	3.046	0.005	3.083	0.053	3.082
Sum	7.971	17.91	7.950	17.926	7.995	17.937
Alman	0.727		0.734		0.730	
Pyrop	0.086		0.086		0.085	
Gross	0.150		0.144		0.148	
Spess	0.037		0.036		0.037	

GARNET-BIOTITE THERMOMETER - Seven calibrations								
RESULTS	(Ref P=3Kb,Temperatures (°C))							
Sample	B92-HW	B92-GS	Dasg-91	FS78	HS82	PL83	T76	HL77
70#1	672	666	708	754	768	669	716	688
70#2	680	672	718	770	785	677	728	698
70#3	699	692	750	810	825	695	755	721
Total average = 721.5 °c								

B92=Bhattacharya et al., 1992; Dasg91=Dasgopta et al., 1991; FS78=Ferry and Speer, 1978; S8 =Hodges and Speer, 1982; PL83=Perchuk and Lavernteva. 1983; T76= Thompson, 1 976; HL77 Holdawayand Lee, 1977.

As noted earlier, the presence of garnet in some samples indicates they were originated from than 45 km depth (13.99 kb), corresponding to deep crustal level in N-SSZ. It shows that the hydrous felsic magmas (Grt- and And- Gr and Gr-Alk Gr) cut the granitic solidus (with different H_2O content) at shallow crustal level then partially melt the surrounding muscovite-bearing crustal components.

As the hornblende is not a stable phase in corundum-normative S-type magmas (Burnham 1992), the presence of hornblende-bearing granites in the field of dehydration melting of muscovite-bearing crustal components (Fig. 6) is also indicate melting of muscovite-bearing sediments may partly provide requisite water for its crystallization from I-type parent magma. This is supported by the presence of micaceous restitic enclaves in the I-type Hbl-granites. This is consistent with both I- and S-type affinity in NW-MPC granitoids, as illustrated by Ahadnejad et al. (2008).

Assuming pressure gradient of 27kb/km, the result of geothermobarometry on NW MBPC granitoids indicates higher geothermal gradient relative to pressure gradient which is not consistent with that reported from normal subduction zone setting. It may indicate local increase in temperature either by crustal thickening or intrusion of mantle-generated mafic magmas beneath LCC in the N-SSZ.

Table 5) The result of P-T estimation by different geothermobarometer relevant to this study. Pem: emplacement pressure, Tcry: crystallization temperature, Grt: garnet, Zr: Zircon, Apt: apatite.

<table>
<tr><td></td><td colspan="2">Pem(kbar)</td><td colspan="6">Tcry (°C)</td></tr>
<tr><td></td><td>Al in hornblende barometer</td><td>Quartz-Albite-Orthos haplogranitic system</td><td colspan="2">Tl-in-Biotite thermometer at P: 4-5kb</td><td>Biotite-garnet thermometer</td><td>Zr and Apt saturation thermometers (Average T(°C))</td><td colspan="2">Amphibole-plagioclase thermometer</td></tr>
<tr><td>Rock type</td><td>Hbl-bearing granitoids</td><td>Hbl-free granitoids</td><td colspan="2">Grt-bearing Monzogranite</td><td>Biotite-garnet-bearing alkali granite</td><td>Hbl-Free granitoids</td><td colspan="2">Hbl-bearing granitoids</td></tr>
<tr><td>Hyperalkalin Granite</td><td>—</td><td>~ 8.5</td><td colspan="2">—</td><td>721.5</td><td>—</td><td colspan="2">—</td></tr>
<tr><td>Quartz Diorite</td><td>2.8 to 3.7</td><td>—</td><td colspan="2">—</td><td>—</td><td>—</td><td colspan="2">661</td></tr>
<tr><td>Monzogranite</td><td>4.26</td><td>3 to 5</td><td>633-659</td><td rowspan="3">mean: 657°C</td><td>—</td><td rowspan="3">> 700 °C 777 and 753 kb</td><td>687</td><td rowspan="3">< 750 °C</td></tr>
<tr><td>Syenogranite</td><td>4.47</td><td><10</td><td>609-634</td><td>—</td><td>649</td></tr>
<tr><td>Granodiorite-Tonalite</td><td>3.68</td><td>0.5 to 5</td><td>633-681</td><td>—</td><td>724</td></tr>
</table>

6- Conclusion

For the samples selected from the NW MBPC granitoids and analyzed for mineral whole-rock chemistry we applied different geothermobarometery method. We achieved relatively three distinct areas of P-T condition for their emplacement: (1) Low- P and T (P< 5kb and T < 680°C) for Garnet- and andalusite-bearing granite (Grt- And Gr) and quartz sample diorite. (2) High- P and T (~ 8 kb and T = 721°C) for garnet-bearing alkali granite (Grt-Alk Gr), and (3)- Low P and high T (P< 5kb and T > 750°C) for hornblende-bearing I-type granite (Hbl-granite) and hornblende-free S-type granite.

Considering the mineralogy and P-T condition of the emplacement for individual phases in the NW MBPC, we concluded that, the parent magmas for I-type granitoids (including hornblende-bearing granites and quartz diorite) were mainly originated from melting of lower crust components and cut the granite solidus at lower pressure. They show little evidence for assimilation of crustal sediments at emplacement level. The parent magmas for S-type granitoids were mainly originated from melting of shallow muscovite-bearing crustal rocks (hornblende-free granites) whereas those originated from higher depth (including garnet-bearing monzogranite, alkali granites) was likely undergone extensive assimilation of crustal components and mixing with melts derived from muscovite-bearing crustal sediments.

Acknowledgements

Special thanks go to Dr. Vahid Ahadnejad for providing the data base, and his constructive suggestions that helped to improve the manuscript.

References

Ahadnejad, V., M.V. Valizadeh, Esmaeily, D. 2008. Shear zone control on the emplacement of Malayer granitoid complex. NW Iran. Journal of Applied Sciences: 8, 23.

Ahadnejad, V., Valizadeh, M.V., Deevsalar, Reza., Rezaei Kahkhaei, Mehdi. 2010. Age and geotectonic position of the Malayer granitoids: Implication for plutonism in the Sanandaj-Sirjan Zone, W Iran. Neues Jahrbuch Für Geologie Und Paläontologie: 261, 61–75.

Ahadnejad, V. 2010. Petrology, geodynamic and emplacement mechanism of Malayer plutonic complex using anisotropic magnetic susceptibility (AMS). PhD Thesis, Tehran University.

Ahadnejad, V. 2013. Comparative review of the Northern Sanandaj-Sirjan Zone granitoids. J Tethys : 1 (2), 128–137.

Ahmadi-Khalaji, A., Esmaeily, D., Valizadeh, M.V., Rahimpour-bonab, H. 2007. Petrology and geochemistry of the granitoid complex of Boroujerd, Sanandaj-Sirjan zone, Western Iran. Journal of Asian Earth Sciences : 29 (5–6), 859–877.

Anderson, J.L., Smith, D.R. 1995. The effects of temperature and fO2 on the Al-in-hornblende barometer. American Mineralogist : 80, 549–559.

Baharifar, A.A., Bellon, H., Pique, A., Moein-Vaziri, H. 2004. The crystalline complexes of Hamadan Sanandaj-Sirjan zone, western Iran): metasedimentary Mesozoic sequences affected by late Cretaceous tectono-metamorphic and plutonic events. Comptes Rendus Geosciences : 336 (16): 1443–1452.

Bea, F., Fershtater, G.B., Corretgé, L.G. 1992. The geochemistry of phosphorus in granite rocks and the effects of aluminium. Lithos: 29, 43–56.

Bhattacharya, A., Mohanty, L., Maji, A., Sen, S.K., Raith, M, 1992. Non-ideal mixing in the phologopite-annite binary: constraints from experimental data on Mg-Fe partitioning and a reformulation of the biotite-garnet geothermometer. Contribution to Mineralogy and Petrology : 111, 87–93.

Braud, J. 1987. La suture du Zagros au niveau de Kermanshah (Kurdistan Iranian): Reconstitution paleogeographique, evolution geodynamique, magmatique et structurale. Ph.D. Thesis, Geodiffusion editeur, Paris, France.

Blundy, J.D., Holland, T.J.B. 1990. Calcic amphibole equilibria and a new amphibole-plagioclase geothermometer. Contribution to Mineralogy and Petrology : 104, 208–224.

Burnham, W. C, 1992. Calculated melt and restite compositions of some. Australian granites. Royal Society of Edinburgh: Earth Sciences: 83, 387–397.

Clemens, J. D. 1984. Water contents of silicic to intermediate magmas. Lithos: 17, 273–287.

Dasgupta, S., Sengupta, P., Dipayan, G., Fukuoka, M. 1991. A refined garnet - biotite Fe−Mg exchange geothermometer and its application in amphibolites and granulites. Contribution to Mineralogy and Petrology : 109, 130–137.

Deevsalar, R. 2009. Petrology and geochemistry of the granitoids from Malayer plutonic complex and their magmatic enclaves and meta-pelittic xenoliths (Western Iran). Unpublished MSc thesis, Tehran University, Iran.

Deevsalar, R., Ghorbani, M. R., Ghaderi, M., Ahmadian, J., Murata, M., Ozawa, H., Shinjo, R. 2014. Geochemistry and petrogenesis of arc-related to intraplate mafic magmatism from the Malayer-Boroujerd plutonic complex, northern Sanandaj-Sirjan magmatic zone, Iran. Neues Jahrbuch für Geology and Paläontology Abh: 274/1, 81–120.

Deevsalar, R., Shinjo, R., Ghaderi, M, Murata., M., Hoskin, P.W.O., Oshiro, S., Wang, K.L., Lee, H.Y., Neill, I. 2017. Mesozoic-Cenozoic mafic magmatism in Sanandaj-Sirjan Zone, Zagros Orogen (Western Iran): geochemical and isotopic inferences from Middle Jurassic and Late Eocene gabbros. Lithos: in press. doi: 10.1016/j.lithos.2017.05.009.

Emami, M.H., Sadeghi M.M., Omrani, S.J. 1994. Magmatic Map of Iran 1:1,000,000. Geological Survey of Iran, internal report.

Esna-Ashari, A., Tiepolo, M., Valizadeh, M.V., Hassanzadeh, J., Sepahi, A.A. 2012. Geochemistry and zircon U–Pb geochronology of Aligoodarz granitoid complex, Sanandaj-Sirjan zone, Iran. Journal of Asian Earth Sciences : 43(1), 11–22.

Ferry, J.M., Spear, F.S. 1978. Experimental calibration of the partitioning of Fe and Mg between biotite and garnet. Contributions to Mineralogy and Petrology : 66, 113–117.

Fornelli, A., Piccarreta, G., Del Moro, A., Acquafreeda, P. 2002. Quantitative models of trace element behavior in magmatic process. Allègre, C.J., Minster, J.F. 1978, Earth and Planetary Science Letter : 38, 1–25.

Hammarstrom, J.M., Zen, E-an. 1986. Aluminium in hornblende: An empirical igneous geobarometer. American Mineralogist : 71, 1297–1313.

Hanchar, J.M., Watson, E.B. 2003. Zircon Saturation Thermometry, In: Zircon, ch. 4, 89–112 (Reviews in Mineralogy and Geochemistry : 53, J.M. Hanchar and P.W.O. Hoskin, Eds.). Mineralogical Society of America, Washington D.C.

Harrison, T.M., Watson, E.B. 1984. The behavior of apatite during crustal anatexis: equilibrium and kinetic considerations. Geochimca Cosmochimca Acta: 48, 1467–1477.

Ghalamghash, J., Nédélec, A., Bellon, H., Vousoughi Abedini, M., Bouchez, J.L. 2009a. The Urumieh plutonic complex (NW Iran): a record of the geodynamic evolution of the Sanandaj–Sirjan zone during Cretaceous times- part I: petrogenesis and K/Ar dating. Journal of Asian Earth Sciences: 35, 401–415.

Ghalamghash, J., Bouchez, J.L., VosoughiAbedini, M., Nédélec, A. 2009b. The Urumieh Plutonic Complex (NW Iran): Record of the geodynamic evolution of the Sanandaj–Sirjan zone during Cretaceous times – Part II: Magnetic fabrics and plate tectonic reconstruction. Journal of Asian Earth Sciences: 36, 303–317.

Grove, T. L., Elkins-Tanton, L. T., Parman, S. W., Chatterjee, N., Müntener, O., Gaetani, G. A. 2003. Fractional crystallisation and mantle-melting controls on calc-alkaline differentiation trends. Contributions to Mineralogy and Petrology: 145, 515–533.

Henry, D.J., Guidotti, C.V., Thomson, J.A. 2005. The Ti-saturation surface for low-to-medium pressure metapelitic biotite: Implications for Geothermometry and Ti-substitution Mechanisms. American Mineralogist: 90, 316–328.

Hodges, K.V., Spear, F.S. 1982. Geothermometry, geobarometry and the

Al_2SiO_5 triple point at Mt. Moosilauke, New Hampshire. American Mineralogist: 67, 1118–1134.

Holdaway, M.J., Lee, S.M. 1977. Fe–Mg cordierite stability in high grade pelitic rocks based on experimental, theoretical, and natural observations, Contributions to Mineralogy and Petrology: 63, 175–198.

Holland, T., Blundy, J. 1994. Non-ideal interactions in calcic amphiboles and their bearing on amphibole-plagioclase thermometry. Contribution to Mineralogy and Petrology: 116, 433–447.

Hollister, L.S., Grissom, G.C., Peters, E.K., Stowell, H.H., Sisson, V.B. 1987. Confirmation of the empirical correlation of Al in hornblende with pressure of solidification of calc-alkaline plutons. American Mineralogist: 72, 231–239.

Hacker, B. R., Mehl, L., Kelemen, P. B., Rioux, M., Behn, M. D. and Luffi, P. 2008. Reconstruction of the Talkeetna intraoceanic arc of Alaska through thermobarometry. Journal of Geophysical Research, Solid Earth: 113, doi:10.1029/2007JB005208.

Huang, W., Wyllie, P. 1975. Melting relations in the system NaAlSi3O8- KAlSi3O8-SiO2 to 35 kilobars, Dry and excess water. Journal of Geology: 83, 737–748.

Hydman, D.W. 1985. Petrology of Igneous and Metamorphic Rocks. NewYork, McGraw-Hill, 533pp.

Janoušek, V., Farrow, C. M. and Erban, V. 2006. Interpretation of whole-rock geochemical data in igneous geochemistry: introducing Geochemical Data Toolkit (GCDkit). Journal of Petrology: 47(6), 1255–1259.

Johnson, M.C., Rutherford, M.J. 1989. Experimental calibration of the aluminium-in hornblende geobarometer with applications to Long Valley caldera (California) volcanic rocks. Geology: 17, 837–841.

Janoušek, V. 2006. Saturnin, R language script for application of accessory-mineral saturation models in igneous geochemistry. Geologica Carpathica: 57, 2, 131–142.

Kawamoto, T. 1996. Experimental constraints on differentiation and H2O abundance of calc-alkaline magmas. Earth and Planetary Science Letters: 144, 577–589.

Kholgi, M.H., Vossoughi Abedini, M. 2005. Petrogenesis, Geodynamics and Radiometric Age Dating of Safakhaneh Mass, Northwest of Iran. Quarterly Geosciences: 66, 24–39.

Lissenberg, C.J, Bedard, J.H., van Staal C.R. 2004. The structure and geochemistry of the gabbro zone of the Annieopsquotch Ophiolite, Newfoundland; implications for lower crustal accretion at spreading ridges. Earth and Planetary Science Letter: 229 (1–2), 105–123.

Luth, W., Jahns, R. Tuttle, O. 1964. The granite system at pressures of 4-10 kbar. Journal of Geophysical Research: 69, 759–773.

Mohajjel, M., Fergusson, C. 2014. Jurassic to Cenozoic tectonics of the Zagros Orogen in northwestern Iran. International Geology Review: 56 (3), 263–287.

Masoudi, F. 1997. Contact metamorphism and pegmatites development in the region SW of Arak, Iran. Ph.D. Thesis, University of Leeds, UK.

Masoudi, F., Yardley, B.W.D., Clif, R.A. 2002. Rb–Sr geochronology of pegmatites, plutonic rocks and a hornfels in the region south-west of Arak, Iran. J. Sci., Islamic Republic of Iran: 13, 249–254.

McCall, G.J.H. 2002. A summary of the geology of the Iranian Makran. - In: Cliff P. D., Kroon D., Gaedecke C. and Craig J. (Eds.): The tectonics and climatic evolution of the Arabian Sea region. Geological Society of London Special Publication: 195, 147–204.

Pattison, D.R.M., Carmichael, D. M., St-Onge, M. R. 1982. Geothermometry and geobarometry applied to Early Protero zoic “S-type” granitoid plutons, Wopmay orogen, Northwest Territories, Canada. Contributions to Mineralogy and Petrology: 79, 394–404.

Perchuk, L.L., Lavrenteva, I.V. 1983. Experimental investigations of the exchange equilibria in the system garnet–cordierite–biotite. Contributions to Mineralogy and Petrology: 99, 226–237.

Petford, N., Atherton, M. 1996. Na-rich partial melts from newly underplated basaltic crust: the Cordillera Blanca Batholith, Peru. Journal of Petrology: 37, 1491–1521.

Pichavant, M., Macdonald, R. 2007. Crystallization of primitive basaltic magmas at crustal pressures and genesis of the calc-alkaline igneous suite: experimental evidence from St Vincent, Lesser Antilles arc. Contributions to Mineralogy and Petrology: 154, 535–558.

Pin, C., Vielzeuf., D. 1983. Granulites and related rocks in Variscan median Europe: a dualistic interpretation. Tectonophysics: 93, 47–74.

Reiners, P.W., Nelson, B.K., Ghiosrso, MS, 1995. Assimilation of felsic crust by basaltic magma: Thermal limits and extents of crustal contamination of mantle-derived magmas. Geology: 23, 563–566.

Schairer, J., Bowen, N. 1935. Preliminary report on equilibrium relations between feldspathoids, alkali feldspars and silica. Transactions of the American Geophysical Union (American Geophysical Union Annual Meeting), 325–328.

Schmidt, M.W. 1992. Amphibole composition in tonalite as a function of pressure: an experimental calibration of the Al-in-hornblende barometer. Contribution to Mineralogy and Petrology: 110, 304–310.

Schmidt, M.W. and Poli, S. 2004. Magmatic Epidote. Reviews in Mineralogy and Geochemistry: 56, 399–430.

Schmidt, M.W. and Thompson, A.B. 1996. Epidote in calc-alkaline magmas: An experimental study of stability, phase relationships, and the role of epidote in magmatic evolution. American Mineralogist: 81, 462–474.

Shahbazi, H., Siebel, W., Pourmoafee, M., Ghorbani, M., Sepahi, A.A., Shang, C.K., Vousoughi-Abedini, M. 2010. Geochemistry and U–Pb zircon geochronology of the Alvand plutonic complex in Sanandaj–Sirjan Zone (Iran): New evidence for Jurassic magmatism. Journal of Asian Earth Sciences: 39(6), 668–683.

Sisson, T.W., Grove, T.L. 1993. Experimental investigations of the role of H2O in calc-alkaline differentiation and subduction zone magmatism. Contributions to Mineralogy and Petrology: 113, 143–166.

Sisson, T.W., RatajeskI, K., Hankins, W.B., Glanzer, A.F. 2005. Voluminous granitic magmas from common basaltic sources. Contributions to Mineralogy and Petrology: 148, 635–661.

Smith, D.R., Leeman, W.P. 1987. Petrogenesis of the Mt. St. Helens dacitic magmas. Journal of Geophysical Research: 92, 10313–10334.

Tatsumi, Y., Suzuki, T. 2009. Tholeiitic vs. calc-alkalic differentiation and evolution of arc crust: constraints from melting experiments on a basalt from the Izu-Bonin Mariana arc. Journal of Petrology: 50, 1575-1603.

Tuttle, O., Bowen, N. 1958. The origin of granite in the light of experimental studies in the system $NaAlSi_3O_8$-$KAlSi_3O_8$-SiO_2-H_2O. Geological Society of America Memoir: 74.

Thompson, A.B. 1976. Mineral reactions in pelitic rocks: II. Calculation of some P–T–X (Fe–Mg) phase reactions, American Journal of Science: 276, 425–454.

Valizadeh, M.V., Cantagrel, J. M. 1975. Premieres donnees radiometriques (K-Ar et Rb-Sr) sur les micas du complexe magmatique du Mont Alvand pres Hamedan (Iran Occidental). Comptes Rendus Hebdomadares des Seances de l'Academie des Sciences, Serie D. Sciences Naturelles: 281, 1083–1086.

Vyhnal, C.R., McSween, H.Y., Speer, J.A., 1991. Hornblende chemistry in southern Appalachian granitoids: implications for aluminumhornblende thermobarometry and magmatic epidote stability. American Mineralogist: 76, 176–188.

Watson, E.B., Harrison. T.M. 1983. Zircon saturation revisited: temperature and composition effects in a variety of crustal magma types. Earth and Planetary Science Letters: 64, 295–304.

Wickham, S.M, 1987. Crustal anatexis and granite petrogenesis during low pressure regional metamorphism; the Trois Seigneurs Massif, PyrenCes, France. Journal of Petrology: 28.

Vielzeuf, D., Holloway, J. R. 1988. Experimental determination of the fluid-absent melting relations in the pelitic system. Consequences for crustal differentiation. Contributions to Mineralogy and Petrology: 98, 257–276.